치의과학석사 학위논문

Anti-cancer effects of genipin in human oral squamous cell carcinoma by inhibiting STAT3 signaling

구강 편평상피세포암종에서 STAT3 신호전달을

억제하는 genipin의 항암 효능에 관한 연구

2023 년 8 월

서울대학교 대학원

치의과학과 구강병리학 전공

박 동 국

Anti-cancer effects of genipin in human oral squamous cell carcinoma by inhibiting STAT3 signaling

구강 편평상피세포암종에서 STAT3 신호전달을

억제하는 genipin의 항암 효능에 관한 연구

지도 교수 조 성 대

이 논문을 치의과학석사 학위논문으로 제출함
2023 년 6 월

서울대학교 대학원
치의과학과 구강병리학 전공
박 동 국

박동국의 치의과학석사 학위논문을 인준함
2023 년 7 월

위 원 장 _____ 윤 혜 정 _____ (인)

부위원장 _____ 홍 성 두 _____ (인)

위 원 _____ 조 성 대 _____ (인)

Abstract

Anti-cancer effects of genipin in human oral squamous cell carcinoma by inhibiting STAT3 signaling

Dong-Guk Park
Program in Oral Pathology
Department of Dental science
The Graduate School
Seoul National University
Supervised by Professor Sung-Dae Cho, D.V.M., Ph.D.

Background: Genipin, which is a natural compound derived from the fruit of Gardenia jasminoides Ellis, was reported to have activity against various cancer types. In this study, I determined the underlying mechanism for genipin-induced apoptotic cell death in human oral squamous cell carcinoma (OSCC).

Methods: The growth inhibitory effects of genipin in human OSCC cells was examined by the Cell Counting Kit-8, soft agar, and cell line-derived xenograft assays. The effects of genipin on apoptotic cell death were assessed by nuclear morphological changes by DAPI staining, measurement of the sub-G1 population, and annexin V-FITC/PI double staining. The underlying mechanism of genipin activity was analyzed by western blotting, subcellular fractionation of the nucleus and cytoplasm, immunocytochemistry, and quantitative real-time PCR.

Results: Genipin inhibited the growth of human OSCC cells both in vitro and in vivo. Genipin also induced apoptotic cell death in human OSCC cells, which was mediated through a caspase-dependent pathway. Genipin reduced phosphorylation of signal transduction and activator of transcription 3 (STAT3) at Tyr705 as well as its nuclear localization. Furthermore, the inhibition of p-STAT3^{Tyr705} levels following genipin treatment was required for the reduction of survivin and myeloid cell leukemia-1 (Mcl-1) expression, which resulted in apoptotic cell death. The genipin-mediated reduction in

survivin and Mcl-1 expression was caused by transcriptional and/or post-translational regulatory mechanisms, which occurred in a cell context-dependent manner.

Conclusions: The results provide insight into the regulatory mechanism by which genipin induces apoptotic cell death through the abrogation of STAT3 phosphorylation within the nucleus and suggest that genipin represents a potential therapeutic option for the treatment of human OSCC.

Keywords: Genipin; Signal transduction and activator of transcription 3; Oral squamous cell carcinoma; Apoptotic cell death; Myeloid cell leukemia-1; Survivin

Student Number: 2021-25862

Table of Contents

List of Figures

1. Introduction

Genipin is a natural compound derived from geniposide, which is isolated from the fruit of Gardenia jasminoides Ellis (Shanmugam et al. 2018). In traditional oriental medicine, it has been used for the treatment of liver disease. Previous studies have shown that genipin exhibits anti-tumor activity against a variety of cancers, including liver, prostate, and lung cancers, both in vitro and in vivo (Fan et al. 2020; Yao et al. 2015; Du et al. 2013). It is effective at inducing autophagic or apoptotic cell death by inhibiting the PI3K/AKT/mTOR axis (Wei et al. 2020); however, the effect of genipin and its regulatory mechanism for inducing apoptotic cell death in human OSCC cells are unclear.

Regulated cell death (RCD) is central to controlling tissue development, homeostasis, and cell fate within living organisms (Tang et al. 2019). Of the various forms of RCD, apoptotic cell death is known to be provoked by mechanisms called the intrinsic or extrinsic pathways, which are mediated by mitochondria and death receptors, respectively (Tower 2015; D'Arcy 2019). In most

cancers, apoptotic cell death is triggered by an imbalance between pro- and anti-apoptotic proteins (Mohammad et al. 2015). Thus, it is not surprising that one well-documented hallmark of cancer is the ability to escape apoptotic cell death, leading to carcinogenesis and cancer development (Hanahan and Weinberg 2011; Fulda 2009). Therefore, the induction of apoptotic cell death has long been proposed as a promising strategy for the treatment of various cancers (Carneiro and El-Deiry 2020) including OSCC.

Signal transducer and activator of transcription 3 (STAT3) is a transcription factor that is phosphorylated in response to stimulation by receptor or non-receptor tyrosine kinases (Mohan et al. 2022). During these events, STAT3 forms homodimers primarily through an interaction of its reciprocal Src homology 2 (SH2) domains, which subsequently translocate to the nucleus where they bind to consensus DNA sequences corresponding to the promotor regions of STAT3 target genes (Yang et al. 2020). Importantly, constitutive STAT3 activity contributes to oncogenesis by influencing anti-apoptotic and pro-inflammatory effects as well as cell transformation (Bowman et al. 2000; Lee et al. 2019;

Grandis et al. 2000; Y. Li et al. 2007; Bromberg et al. 1999). In particular, aberrant hyperactivation of STAT3 has been documented in multiple cancers, such as head and neck squamous cell carcinoma (HNSCC), which often correlates with an unfavorable prognosis (D. E. Johnson et al. 2020; Daniel E. Johnson, O'Keefe, and Grandis 2018). Therefore, targeting phosphorylated STAT3 may represent an effective strategy for treating cancer.

In this study, I identified a regulatory mechanism associated with apoptotic cell death in human OSCC cells following genipin treatment, suggesting that genipin may be an attractive therapeutic agent for treating human OSCC.

2. Material & Methods

2.1. Cell culture and pharmacological chemicals

HN22 and HSC-4 cell lines were kindly provided by Dankook University (Cheonan, Republic of Korea) and Hokkaido University (Hokkaido, Japan), respectively. Cells were cultured in DMEM/F-12 medium (WELGENE, Gyeongsan, Republic of Korea) containing 10% fetal bovine serum (FBS) and 1% penicillin/streptomycin (P/S) in a humidified atmosphere at 37° C with 5% CO_2. The experiments were initiated when the cells reached 45-55% confluence. Genipin was purchased from Sigma-Aldrich (#G4796, St. Louis, MO, USA), dissolved in dimethyl sulfoxide (DMSO), and stored at -20℃. The final concentration of DMSO did not exceed 0.1%. Z-VAD-FMK, a pan-caspase inhibitor, was purchased from R&D Systems (Minneapolis, MN, USA). The protein synthesis inhibitor, cycloheximide (CHX), was purchased from Sigma-Aldrich (St. Louis, MO, USA) and the proteasome inhibitor, MG132, was obtained from Santa Cruz Biotechnology (Santa Cruz, CA, USA).

2.2. Cell Counting Kit-8 (CCK-8) assay

Cell viability was measured by the CCK-8 assay (Dojindo Laboratories, Kumamoto, Japan) according to the manufacturer' s protocol. Briefly, cells were seeded into 96-well plates overnight and treated with the indicated concentrations of genipin for 24 h. Next, CCK-8 solution (10 μL) was added to each well and incubated at 37° C with 5% CO_2 for 2 h. The absorbance at 450 nm was measured using a microplate reader (Hidex, Turku, Finland).

2.3. Soft agar colony formation assay

Six-well plates were filled with 3 mL of 1.25% agar mix, treated with the indicated concentrations of genipin, and allowed to solidify at room temperature (RT) for 1-2 h. Cells were prepared by suspending in 10% BME and mixing with agar. Thereafter, 1 mL of cells mixed with genipin was directly added to the solidified bottom agar in 6-well plates, allowed to solidify for 1-2 h at RT, and incubated in a humidified 37° C incubator containing 5% CO_2 for 14 days. Genipin was added to the top or bottom agar and 20 ng/mL Human EGF Recombinant Protein (Thermo Fisher Scientific,

Waltham, MA, USA) was either added to or not added to HN22 or HSC-4, respectively. The colonies were imaged using a CKX53 microscope (Olympus, Tokyo, Japan) and counted with ImageJ software (National Institute of Health, Bethesda, MD, USA).

2.4. Cell line-derived xenograft (CDX) mouse model

HN22 cells suspended in VitroGel® STEM (TheWell Bioscience, North Brunswick Township, NJ, USA) were subcutaneously injected into the flanks of 4-week-old male Balb/c nude mice (NARA-Biotech, Pyeongtaek, Republic of Korea). Approximately 9 days after inoculation, the mice were randomly divided into two subgroups (n = 4 for each group): (i) vehicle control group and (ii) genipin (30 mg/kg/day, intraperitoneal injection 5 times per week for 4 weeks, #G4796, Sigma-Aldrich, St. Louis, MO, USA) treatment group. Tumor volume and body weight were measured twice per week and the mice were sacrificed on day 28 after treatment to measure tumor weight. Tumor volumes were measured along the two diameter axes with calipers and were calculated according to the following formula: $V = \pi/6 \times \{(D + d)/2\}^3$,

where D and d represent the larger and smaller diameters, respectively. All animal procedures were performed by the Institutional Animal Care and Use Committee (IACUC) guidelines approved by CHA University (IACUC approval number: IACUC220062). The standard animal care and laboratory guidelines were followed using the IACUC protocol.

2.5. Evaluation of nuclear morphological changes

DAPI solution (Sigma-Aldrich, St. Louis, MO, USA) was used to determine changes in nuclear condensation and fragmentation within apoptotic cells. Briefly, cells were treated with various concentrations of genipin. The cells were harvested, including detached cells, and fixed with 70% ethanol at −20° C overnight. The cells were resuspended in 100% methanol at RT for 10 min, deposited onto glass slides, and stained with 2 μg/mL DAPI solution in the dark. The stained cells were visualized by fluorescence microscopy (Leica DMi8; Leica Microsystems GmbH, Wetzlar, Hesse, Germany).

2.6. Measurement of sub-G_1 population

Cells were fixed with 70% ethanol overnight at −20° C. After removing the supernatant, the cells were stained with propidium iodide (PI) solution, including 20 μg/mL of RNase A, for 15 min at 37° C. The cell cycle distribution was determined using a FACSCalibur flow cytometer (BD Biosciences, San Jose, CA, USA) and the proportion of stained DNA content was visualized using BD CellQuest™ Pro software. The relative DNA distribution was analyzed using FlowJo software (FlowJo LLC, Ashland, OR, USA).

2.7. Annexin V-FITC/PI double staining

Cells undergoing an early or late stage of apoptotic cell death were measured using the FITC-Annexin V Apoptosis Detection Kit (BD Biosciences, San Jose, CA, USA) according to the manufacturer's protocol. Briefly, harvested cells were resuspended in 400 μL of Annexin V binding buffer, containing 5 μL of FITC-conjugated Annexin V and 1 μL of propidium iodide solution, at RT in the dark. The stained cells were analyzed using LSRFortessa X-20 (BD

Biosciences, San Jose, CA, USA) and the cell population within each compartment was calculated using FlowJo software.

2.8. Western blot analysis

Cells were lysed with RIPA lysis buffer (Millipore, Burlington, MA, USA) supplemented with protease inhibitors (Roche, Mannheim, Germany) and phosphatase inhibitors (Thermo Fisher Scientific, Rockford, IL, USA). Total protein concentrations were determined using the *DC* Protein Assay Kit (Bio-Rad Laboratories, Madison, WI, USA) followed by separation on sodium dodecyl sulfate-polyacrylamide gel electrophoresis (SDS-PAGE) gels and transfer to polyvinylidene difluoride (PVDF) membranes. After blocking with 5% skim milk (#232100, BD Difco™, San Jose, CA, USA) for 2 h at RT, the membranes were incubated with the indicated primary antibodies overnight at 4° C, followed by the corresponding horseradish peroxidase (HRP)-conjugated secondary antibodies (1:2000, catalog #: GTX213110-01 or GTX213111-01, GeneTex, Irvine, CA, USA) for 2 h at RT. The immunoreactive signals were visualized using WestGlow™ PICO PLUS Chemiluminescent

Substrate (BIOMAX, Seoul, Republic of Korea) on X-ray film or with the Image Quant LAS 500 system (GE Healthcare Life Sciences, Piscataway, NJ, USA). Densitometric analyses were carried out using ImageJ software. The primary antibodies used were as follows: STAT3 (1:1000, #4904), p-STAT3^{Tyr705} (1:2000, #9145), p-STAT3^{Ser727} (1:2000, #9134), cleaved PARP (1:2000, #9541), cleaved caspase 3 (1:1000, #9664), survivin (1:1000, #2802), Mcl-1 (1:1500, #5453), and Bcl-XL (1:5000, #2764) were purchased from Cell Signaling Technology (Charlottesville, VA, USA). Bcl-2 (1:1000, #sc-7382), β-actin (1:3000, #sc-47778), and α-tubulin (1:5000, #sc-5286) were obtained from Santa Cruz Biotechnology (Dallas, TX, USA). Histone H3 (1:5000) was kindly provided by Kangwon National University (Chuncheon, Republic of Korea).

2.9. Subcellular fractionation of the nucleus and cytoplasm

Nuclear and cytoplasmic proteins were extracted using the NE-PER^{TM} Nuclear and Cytoplasmic Extraction Reagents Kit (Thermo Fisher Scientific, Rockford, IL, USA). Briefly, the harvested cells

were vortexed with Cytoplasmic Extraction Reagent I, followed by incubation on ice for 10 min. The cells were resuspended in Cytoplasmic Extraction Reagent II for 1 min and centrifuged for 5 min at 13,000 g. The supernatant containing cytoplasmic proteins was transferred to a pre-chilled EP tube (the cytoplasmic fraction). The precipitated pellets were resuspended in Nuclear Extraction Reagent for 40 min, vortexed at 10 min intervals, and thoroughly sonicated. The solution was centrifuged for 10 min at 13,000 g. Finally, the supernatant consisting of nuclear proteins (the nuclear fraction) was collected for western blot analysis.

2.10. Immunocytochemistry

Cells were seeded into 4-well chamber slides and treated with DMSO or genipin. After 24 h, the cells were washed with PBS and fixed with Cytofix/Cytoperm™ solution (BD Biosciences, San Jose, CA, USA) for 1 h at 4° C. The slides were blocked with 1% bovine serum albumin (BSA) at RT for 1 h and incubated with $pSTAT3^{Tyr705}$ antibody (1:100) at 4° C overnight. After washing three times with PBS, the cells were incubated with Alexa Fluor™

488 anti-rabbit antibody (1:150, #A-11034, Invitrogen, Waltham, MA, USA) for 1 h in the dark. The samples were mounted using UltraCruz® Aqueous Mounting Medium with DAPI (Santa Cruz Biotechnology, Santa Cruz, CA, USA). Finally, cells were visualized using an LSM700 confocal laser scanning microscope (Carl Zeiss, Oberkochen, Germany).

2.11. Quantitative real-time PCR (qPCR)

Total RNA was prepared using TRIzol reagent (Life Technologies, Carlsbad, CA, USA) and the amount of extracted RNA was measured using the NanoPhotometer N50 (IMPLEN, Westlake Village, CA, USA). The AMPIGENE cDNA Synthesis Kit (Enzo Life Sciences, Farmingdale, NY, USA) was used to reverse-transcribe 1 μg of total RNA and the resulting cDNA was subjected to qPCR using the AMPIGENE qPCR Green Mix Hi-Rox (Enzo Life Sciences, Farmingdale, NY, USA) with the StepOnePlus™ Real-Time PCR System (Applied Biosystems, Foster City, CA, USA). The PCR conditions for all genes were as follows: 95° C for 2 min, followed by 40 cycles of 95° C for 10 sec, and 60° C for 30 sec. The

relative expression of each gene was determined by the $2^{-\Delta\Delta Ct}$ method and normalized to the amount of GAPDH as an internal control. All primers were synthesized by Cosmo genetech (Seoul, Republic of Korea) and the primer sequences were as follows: Mcl-1 *(Accession number: NG_029069.1)* sense 5′-GTA TCA CAG ACG TTC TCG TAA GG-3′, Mcl-1 5′-CCA CCT TCT AGG TCC TCT ACA T-3′, survivin *(Accession number: NG_029146.2)* sense 5′-ACT TGG CCC AGT GTT TCT T-3′, survivin anti-sense 5′-GAC AGA AAG GAA AGC GCA AC-3′, GAPDH *(Accession number: NG_007073.2)* sense 5′-GTG GTC TCC TCT GAC TTC AAC-3′, GAPDH anti-sense 5′-CCT GTT GCT GTA GCC AAA TTC-3′.

2.12. Statistical analysis

All graphs were constructed using GraphPad Prism version 8.4.2 (GraphPad Software, San Diego, CA, USA) and all statistical tests were conducted using SPSS version 25.0 (SPSS, Chicago, IL, USA). All data are presented as the mean ± standard deviations (SD) from at least three independent experiments. For in vitro studies,

two variables were compared using a two-tailed student's *t*-test, whereas a one-way ANOVA analysis was performed for multiple comparisons along with Tukey's post hoc test. For in vivo studies, non-normally distributed datasets were analyzed using the nonparametric Mann-Whitney test. For all cases, the statistical significance was set at $p < 0.05$ (* or #).

3. Results

3.1. Genipin inhibits the tumorigenesis of human OSCC both in vitro and in vivo

To determine the anticancer effect of genipin on human OSCC, the CCK-8 assay was performed to assess cell viability in two human OSCC cell lines (HN22 and HSC-4) following genipin treatment. As shown in Fig. 1A, a 24 h exposure to genipin significantly decreased cell viability in both cell lines in a concentration-dependent manner. The IC_{50} values for HN22 and HSC-4 cells were 128 ± 26 μM and 111 ± 10 μM, respectively. Similarly, clonogenic growth in genipin-treated cells was much lower compared with that in DMSO-treated cells, as evidenced by a reduction in both colony number and size (Fig. 1B). To determine the effect of genipin on tumor progression in human OSCC in vivo, I used the CDX mouse model by injecting HN22 cells subcutaneously into the flanks of Balb/c nude mice. As shown in Fig. 2A and 2B, the tumor volume of the genipin-treated group after 24 and 28 days was reduced

compared with that of the vehicle control group (p = 0.029). There were no significant differences in body weight between the vehicle control and genipin treatment groups (Fig. 2C). These results indicate that genipin potently inhibits the growth of human OSCC in vitro and in vivo.

3.2. Genipin induces apoptotic cell death in human OSCC cells through a caspase-dependent pathway

To determine whether the cytotoxic effects of genipin are attributed to the induction of apoptotic cell death in human OSCC cells, I analyzed morphological changes, including nuclear condensation, by DAPI staining. As shown in Fig. 3A, genipin induced a marked accumulation of apoptotic cells, as indicated by the white arrows, compared with the control cells. Moreover, genipin treatment not only resulted in the accumulation of cells in the sub-G1 phase (Fig. 3B), but also increased the population within the annexin V-positive compartments (Fig. 3C), indicating induction of apoptotic cell death. The apoptotic effect of genipin was

further verified by western blot analysis, in which genipin treatment markedly induced cleavage of both caspase 3 and PARP (Fig. 4A), which are classic apoptosis markers. Furthermore, I observed that combined treatment with genipin and the pan-caspase inhibitor Z-VAD-FMK abolished cleavage of both caspase 3 and PARP in both cell lines compared with genipin treatment alone (Fig. 4B). These results indicate that genipin promotes apoptotic cell death in human OSCC cells through a caspase-dependent pathway.

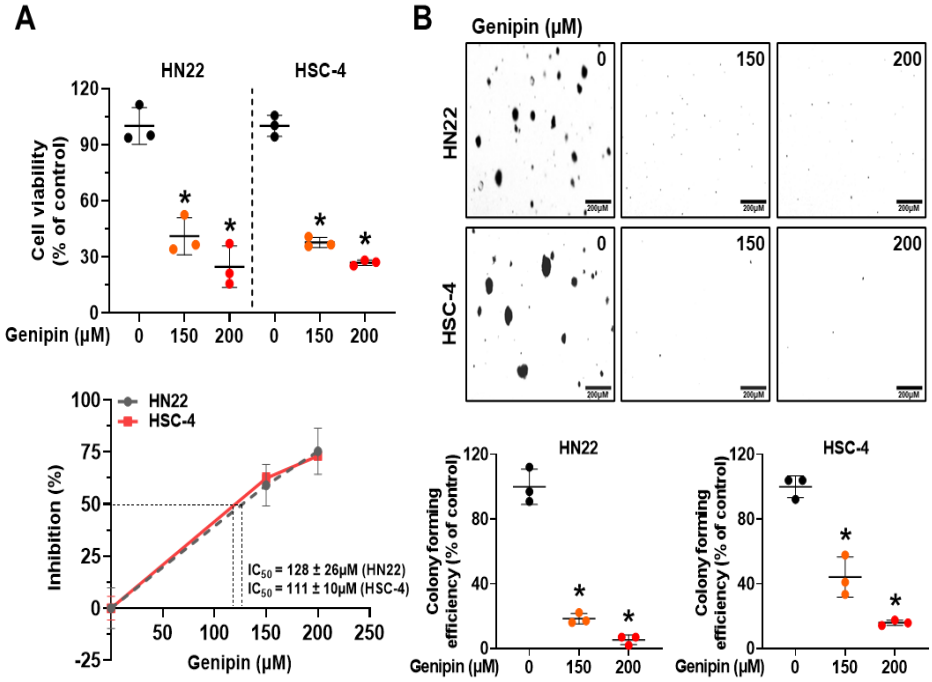

Fig. 1. Effects of genipin on the progression of human OSCC in vitro. Cells were treated with the indicated concentrations of genipin for 24 h. (A) The CCK-8 assay was used to assess the viability of both cell lines treated with either DMSO or genipin (top panel). The IC_{50} values of genipin (bottom panel). (B) Representative images of a soft agar colony formation assay. Magnification, ×40; scale bar, 200 μm. Colonies were automatically counted using ImageJ software. All graphs represent the mean ± SD of triplicate experiments. Significance difference compared to the control group is indicated (*, $p < 0.05$).

A

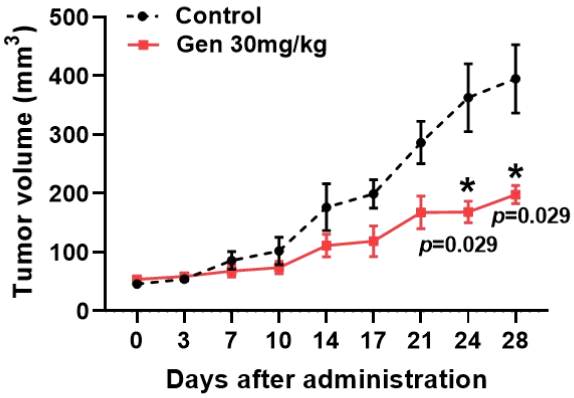
Control
Gen 30mg/kg
Tumor volume (mm3)
500
400
300
200
100
0
0 3 7 10 14 17 21 24 28
Days after administration
*
*
p=0.029
p=0.029

B

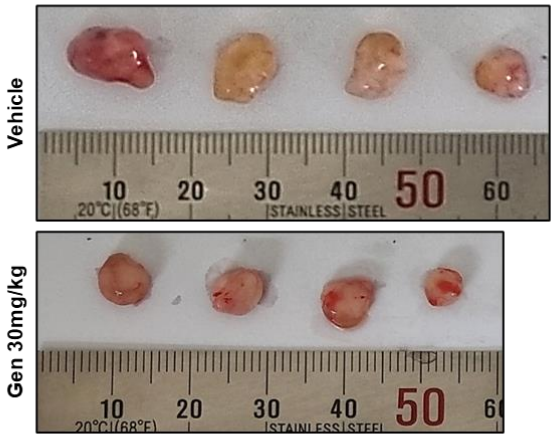
Vehicle
Gen 30mg/kg
10 20 30 40 50 60
STAINLESS STEEL

C

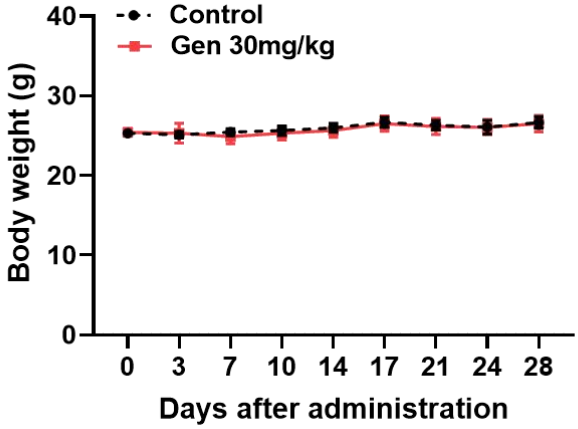
Control
Gen 30mg/kg
Body weight (g)
40
30
20
10
0
0 3 7 10 14 17 21 24 28
Days after administration

Fig. 2. Effects of genipin on the progression of human OSCC in vivo. (A) The tumor volume (B) Representative images of tumors, (C) body weight of the mice was measured. All graphs represent the mean ± SEM. Significance difference compared to the control group is indicated (*, $p < 0.05$).

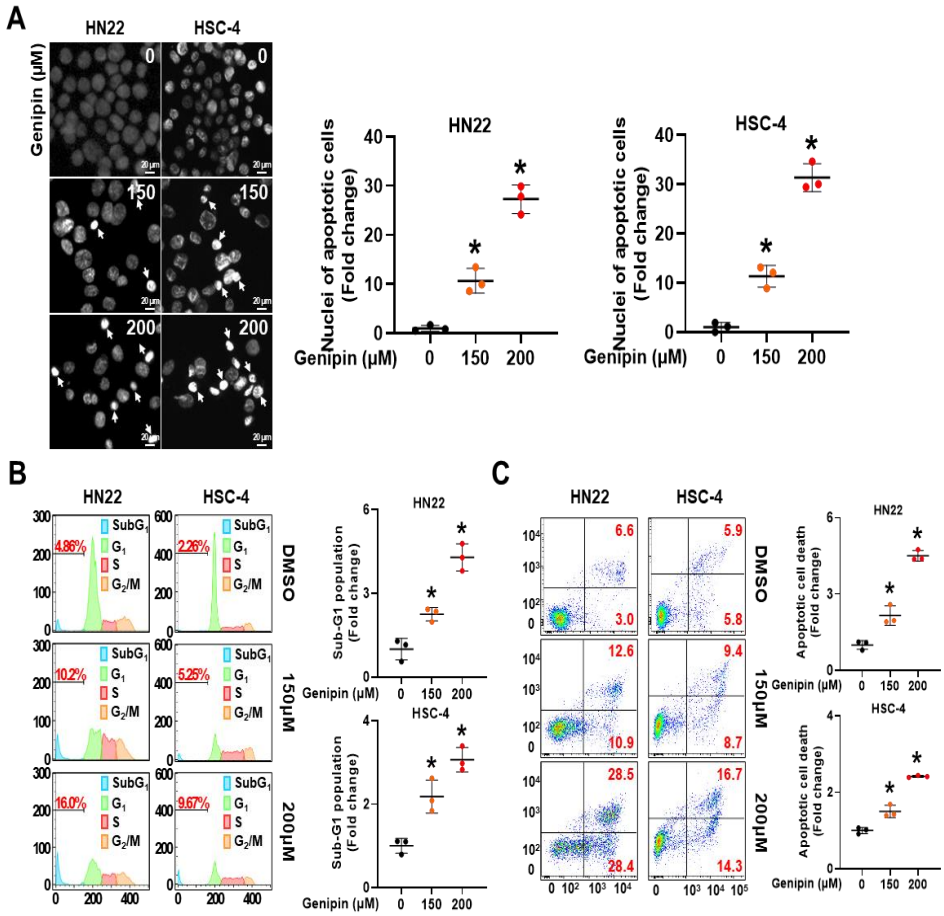

Fig. 3. Effect of genipin on apoptotic cell death in human OSCC cells. (A) Representative image of cells stained with DAPI. Apoptotic cells with nuclear condensation are indicated by white arrows. Magnification, ×400; scale bar, 20 μm. (B) Flow cytometry images of PI-stained cells showing cell cycle distribution. Graphs represent the fold-change of the sub-G1 population in each group. (C) Representative images of annexin V/PI double staining. Graphs

represent the fold-change of apoptotic cells within annexin V-positive compartments. All data represent the mean ± SD of three independent experiments. Significance difference compared to the control group is indicated (*, $p < 0.05$).

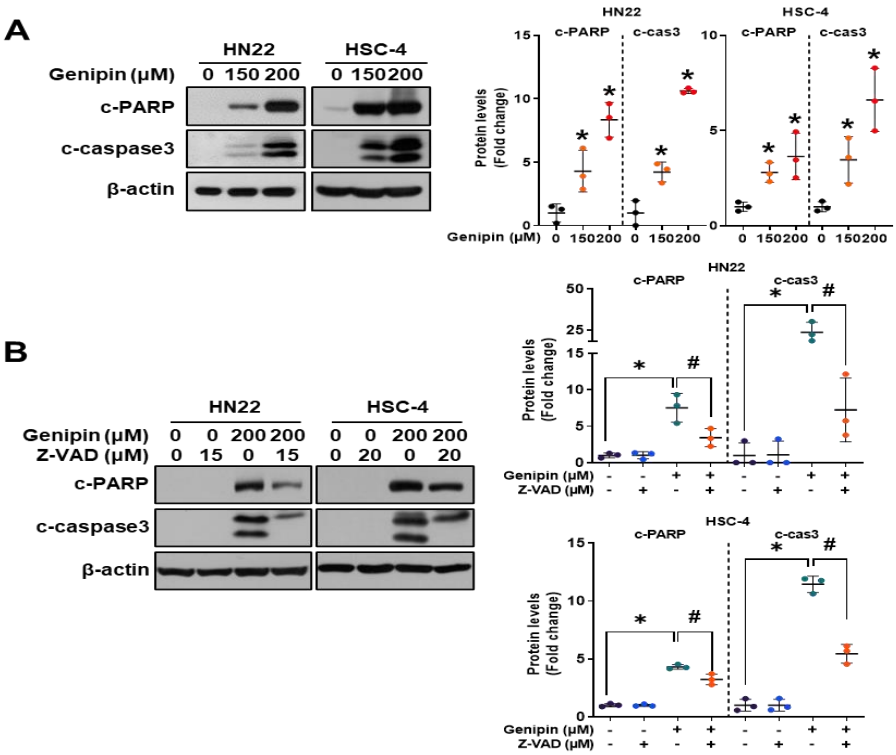

Fig. 4. The role of caspase on genipin-mediated apoptosis.

(A) Western blot analysis showing the expression levels of c-caspase 3 and c-PARP. β-actin was used as an internal control. Significance difference compared to the control group is indicated (*, $p < 0.05$). (B) Cells were pre-treated with Z-VAD-FMK for 1 h, followed by treatment with genipin for 24 h. All data represent the mean ± SD of three independent experiments. * , $p < 0.05$ compared with DMSO treatment alone; # , $p < 0.05$ compared with genipin treatment alone.

3.3. Genipin suppresses STAT3 phosphorylation and its nuclear localization in human OSCC cells

STAT3 functions as a key modulator of several biological processes, including proliferation and apoptotic cell death, in various types of cancer (Baek et al. 2016; Horiguchi et al. 2010; Hu et al. 2021). Previous study suggested that STAT3 phosphorylation was significantly higher in human OSCC tumors compared with that in the normal oral mucosa (Kim et al. 2017). Therefore, I determined whether genipin can suppress STAT3 phosphorylation in human OSCC. As shown in Fig. 5, genipin markedly downregulated STAT3 phosphorylation at Tyr^{705}, but not Ser^{727}, in both cell lines, which indicates that genipin selectively inhibits STAT3 phosphorylation at Tyr^{705} residue only. Furthermore, genipin reduced the expression of $p-STAT3^{Tyr705}$, which predominantly occurred in the nucleus (Fig. 6A). These findings were further supported by immunocytochemistry, in which reduced $p-STAT3^{Tyr705}$ expression was observed predominantly within the nucleus following genipin treatment (Fig. 6B). These results demonstrate that genipin

abolishes p-STAT3^{Tyr705} expression within the nucleus.

3.4. Reduced STAT3^{Tyr705} levels by genipin treatment modulates survivin and Mcl-1 expression to induce apoptotic cell death

To identify which downstream target molecules in the apoptosis pathway are regulated by reduced STAT3 phosphorylation following genipin treatment, I performed western blot analysis to measure survivin, Mcl-1, Bcl-2, and Bcl-XL protein expression. As shown in Fig. 7, the expression of survivin and Mcl-1 was markedly decreased in genipin-treated cells compared with the controls; however, there were no significant differences in Bcl-2 and Bcl-XL levels. Based on these results, I determined whether these two downstream target molecules were attenuated by the reduction of STAT3 phosphorylation following genipin treatment. The expression of p-STAT3^{Tyr705} was abolished in both cell lines at 0.75 h following genipin treatment (Fig. 8). Survivin expression was significantly decreased in both cell lines at 3 h after genipin treatment, whereas Mcl-1 was decreased in HN22 and HSC-4

cells after 6 and 3 h, respectively. Furthermore, a significant increase in c-PARP levels was observed in HN22 and HSC-4 cells at 12 and 6 h post-treatment, respectively. The results indicate that genipin-induced apoptotic cell death in human OSCC cells may be attributed to the sequential reduction of survivin and Mcl-1 expression through inhibition of STAT3 phosphorylation.

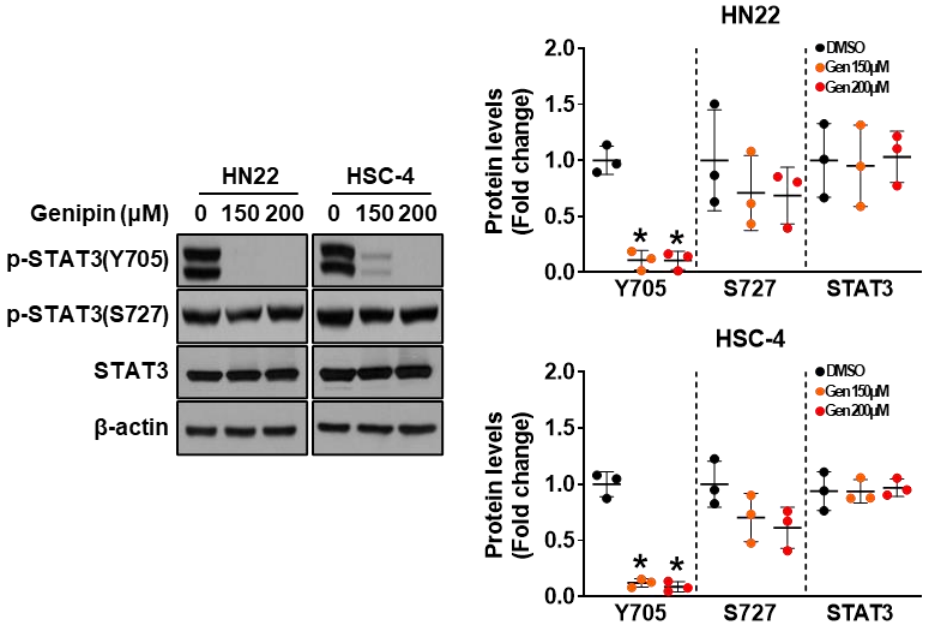

Fig. 5. Effects of genipin on STAT3 phosphorylation in human OSCC cells.

The expression levels of p−STAT3^{Tyr705}, p−STAT3^{Ser727}, and total STAT3 were determined by western blot analysis. β−actin was used as an internal control. All analyses were performed three times independently and the graphs represent the mean ± SD. Significance difference compared to the control group is indicated (*, $p < 0.05$).

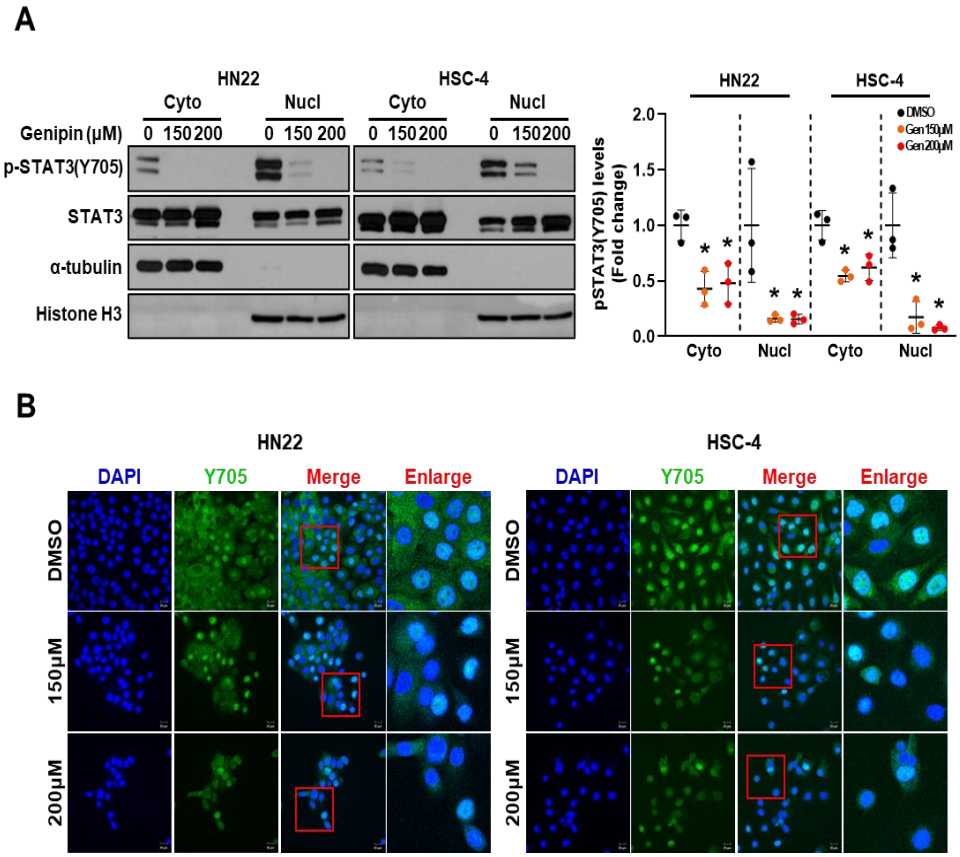

Fig. 6. Effects of genipin on STAT3 nuclear localization in human OSCC cells.

((A) Cytoplasmic and nuclear fractions were prepared to determine the subcellular localization of p-STAT3^{Tyr705}. Histone H3 and α-tubulin were used as specific markers for the nucleus and cytoplasm, respectively. All analyses were performed three times independently and the graphs represent the mean ± SD.

Significance difference compared to the control group is indicated (*, $p < 0.05$). **(B)** Representative images of immunocytochemistry showing the expression levels of p−STAT3^{Tyr705} and its nuclear localization. Fluorescence signals for p−STAT3^{Tyr705} (green) and nuclei counterstained with DAPI (blue) were detected by confocal microscopy. Merged panels of the two images. The red line boxed area is enlarged in the right. Magnification, ×400; scale bar, 20 μm.

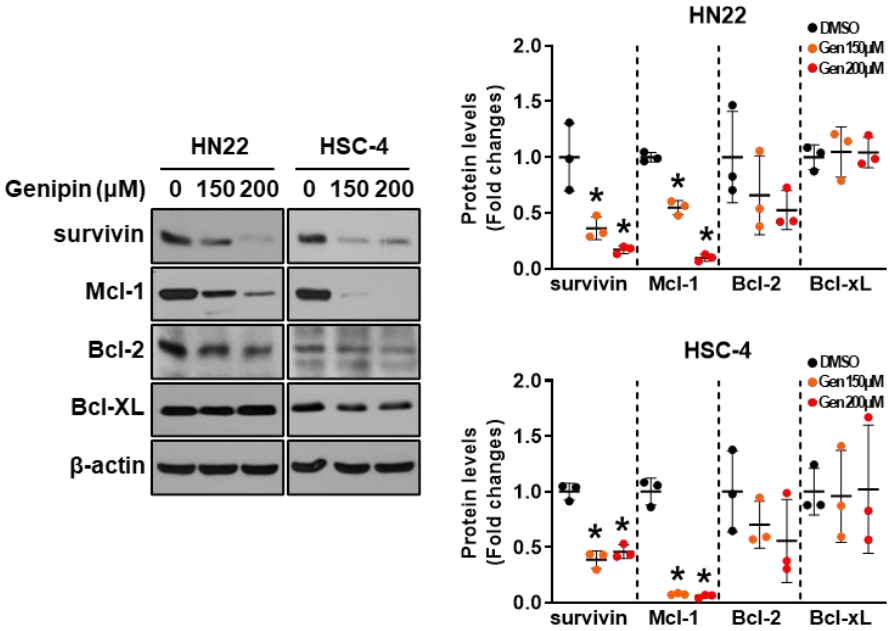

Fig. 7. Reduction of survivin and Mcl−1 expression induced by genipin treatment in human OSCC cells.

Cells were treated with the indicated concentrations of genipin for 24 h. The expression levels of survivin, Mcl−1, Bcl−2, and Bcl−XL were analyzed by western blot analysis. All analyses were performed three times independently and the graphs represent the mean ± SD. Significance difference compared to the control group is indicated (*, $p < 0.05$).

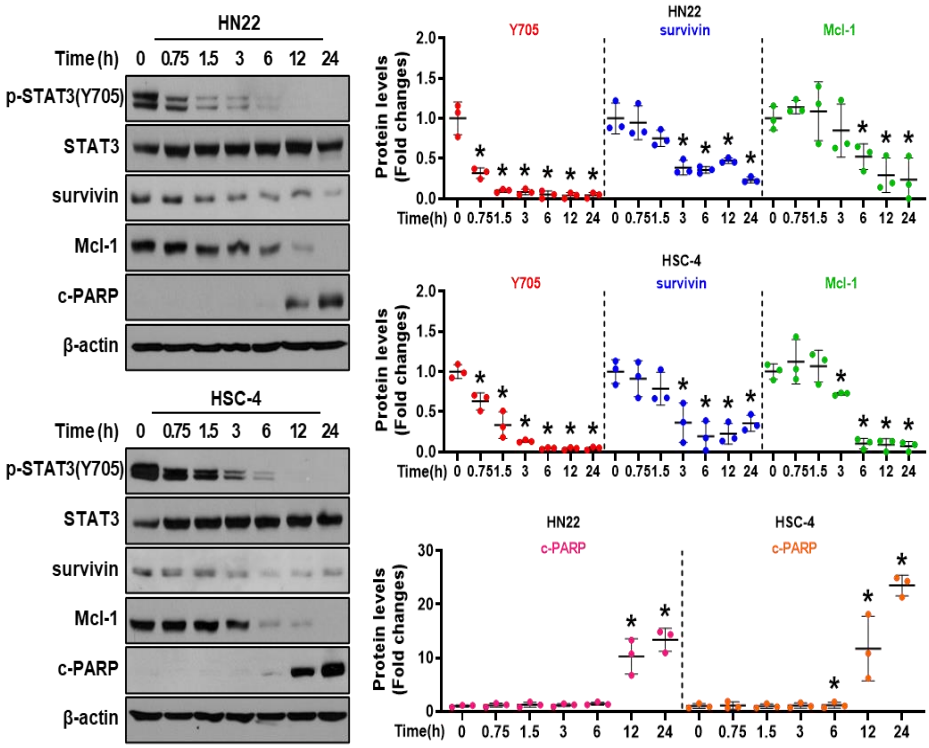

Fig. 8. Association between the expression of STAT3^{Tyr705} and its target genes to induce apoptotic cell death.

Cells were treated with 200 μM of genipin at the indicated time points. Western blot images showing the expression levels of p-STAT3^{Tyr705}, total STAT3, survivin, Mcl-1, and c-PARP. β-actin was used as an internal control. All analyses were performed three times independently and the graphs represent the mean ± SD. Significance difference compared to the control group is indicated (*, $p < 0.05$).

3.5. Genipin modulates survivin and Mcl-1 expression through transcriptional and/or post-translational regulation mechanisms

To further clarify the regulatory mechanisms of survivin and Mcl-1 that were reduced by genipin treatment, I measured survivin and Mcl-1 mRNA expression by qPCR. As shown in Fig. 9, the expression of survivin was suppressed in both cell lines; however, Mcl-1 expression was significantly decreased in HN22 cells at 6 to 24 h following genipin treatment, whereas both exhibited a significant difference in HSC-4 cells at 24 h only. To determine whether the genipin-mediated inhibition of Mcl-1 expression in HSC-4 cells was attributed to reduced protein stability, HSC-4 cells were pre-treated with cycloheximide (CHX), a protein synthesis inhibitor. The results indicated that Mcl-1 expression in cell treated with CHX and genipin was gradually reduced compared with CHX treatment alone (Fig. 10A). Furthermore, the reduced expression of Mcl-1 following genipin treatment was restored by the proteasome inhibitor MG132, which indicates proteasomal degradation of Mcl-1, but not the lysosome inhibitor CQ (Fig. 10B

and 10C). These results demonstrate that genipin alters the expression of survivin and Mcl-1 in human OSCC cells in a cell context-dependent manner through transcriptional and/or post-translational regulatory mechanisms.

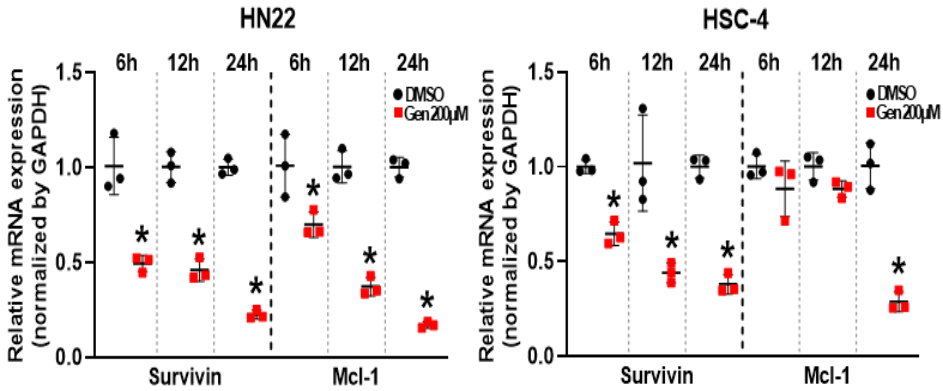

Fig. 9. Transcriptional regulation of survivin and Mcl−1 induced by genipin treatment.

Cells were treated with DMSO or 200 μM of genipin for the indicated times. The relative mRNA levels of survivin and Mcl−1 were assessed by qPCR. All analyses were performed three times independently and the graphs represent the mean ± SD. Significance difference compared to the control group is indicated (*, $p < 0.05$).

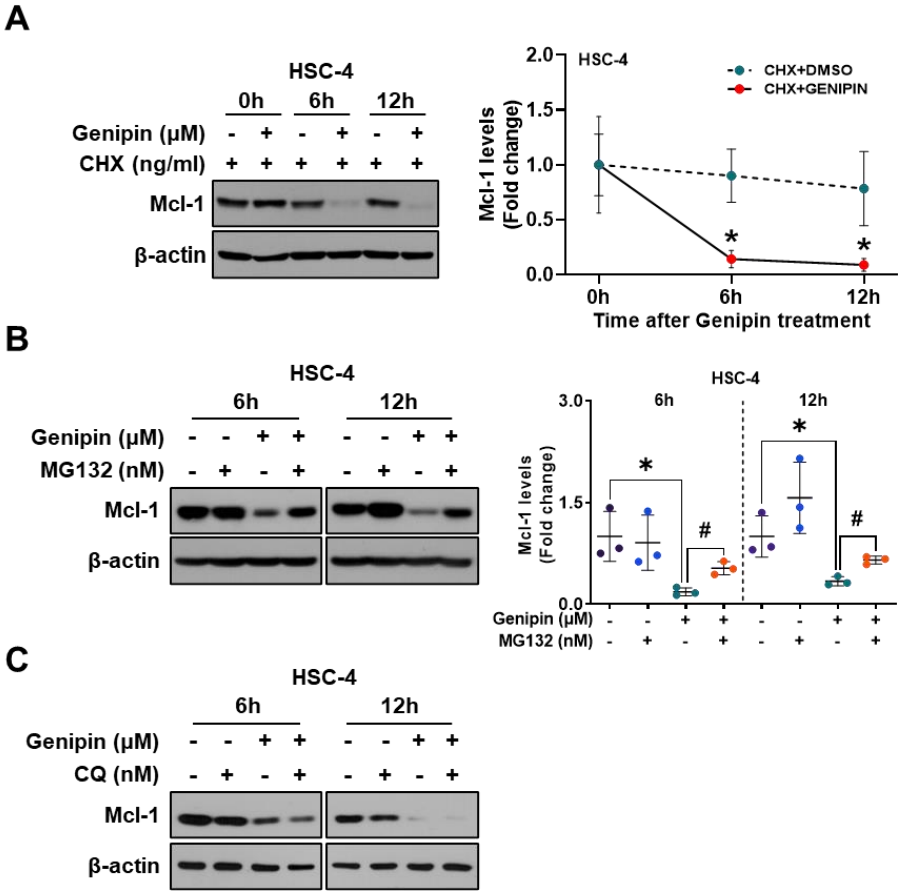

Fig. 10. Post-translational regulation of Mcl-1 induced by genipin treatment.

(A) HSC-4 cells were pre-treated with 50 ng/mL of CHX, a protein synthesis inhibitor, for 1 h before treatment with 200 μM of genipin for the indicated times. Western blot images showing the expression of Mcl-1. Significance difference compared to the control group is indicated (*, $p < 0.05$). (B) HSC-4 cells were pre-

treated with 300 nM MG132, a proteasome inhibitor, for 1 h before treatment with 200 μM of genipin for the indicated times. The expression levels of Mcl-1 were determined by western blot analysis. β-actin was used as an internal control. All analyses were performed three times independently and the graphs represent the mean ± SD. *, $p < 0.05$ compared with DMSO treatment alone; $^{\#}$, $p < 0.05$ compared with genipin treatment alone. (C) HSC-4 cells were pre-treated with 60 nM CQ, a lysosome inhibitor, for 1 h before treatment with 200 μM of genipin for the indicated times.

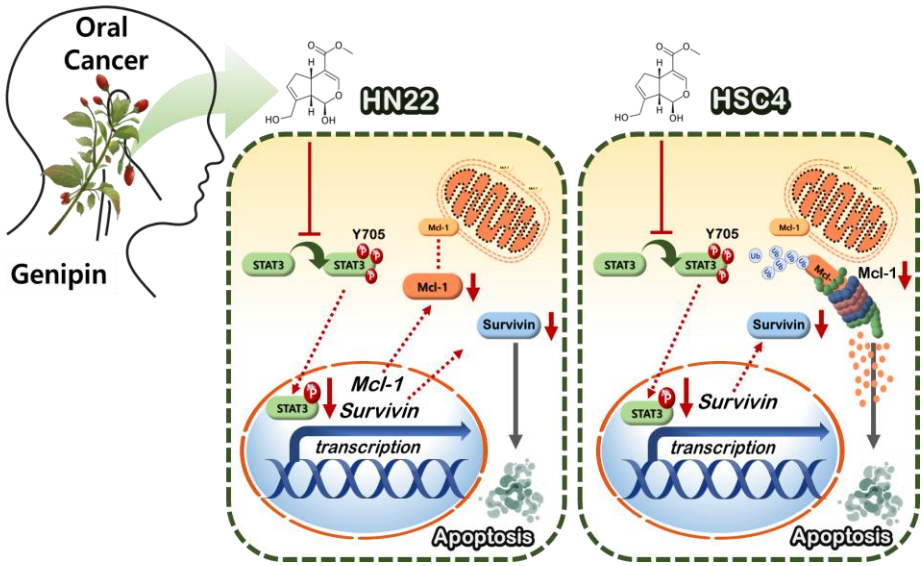

Fig. 11. Working model depicting the molecular mechanism of genipin as a potential STAT3 inhibitor in human OSCC cells.

4. Discussion

STAT3 plays an important role in regulating cell proliferation and anti-apoptotic cell death through transcriptional regulation of various genes (Siveen et al. 2014). Translocation of phosphorylated STAT3 into the nucleus is associated with a worse outcome in cancer patients (Macha et al. 2011); thus, STAT3 has been proposed as an attractive target for cancer treatment (Tu et al. 2011; You et al. 2012). Based on these findings, several compounds that abrogate the expression or activity of STAT3 are being tested pre-clinically and clinically, which act as direct and indirect inhibitors, respectively (L. Sun et al. 2022; McLornan et al. 2021; Jung et al. 2022). In the present study, I found that genipin markedly decreased STAT3 activity in vitro; however, it remains unclear if genipin abrogates STAT3 activity through binding to the SH2 domains, similar to the mechanism underlying other small STAT3 inhibitors or by inhibiting upstream molecules, such as EGFR, JAK, and Src (Siveen et al. 2014; Daniel E. Johnson, O'Keefe, and Grandis 2018). This raises the possibility that the inhibition of

STAT3 activity is likely an effective strategy to slow the progression of human OSCC. Constitutively active STAT3 contributes to therapeutic challenge of conventional treatments as well as an EGFR inhibitor, Cetuximab, an FDA-approved monoclonal antibody (Chen et al. 2021; S. Sun et al. 2018; Zheng et al. 2021). Considering these observations, cancer therapy using the above methods in combination with genipin may result in a favorable outcome for cancer patients harboring tumors with high STAT3 kinase activity.

Constitutively activate STAT3 is associated with the upregulation of survivin in gastric cancer cells and primary effusion lymphoma (Kanda et al. 2004; Aoki, Feldman, and Tosato 2003). Moreover, survivin is significantly overexpressed in OSCC patients and high expression is associated with worse survival rates (Lo Muzio et al. 2003; M. Li et al. 2020). Survivin is regulated by transcriptional, translational, and post-translational processes (Boidot, Vegran, and Lizard-Nacol 2014; Wheatley and Altieri 2019). Of these, transcriptional regulation of survivin occurs by several transcription factors, including STAT3, HSF-1α, and Sp1 (Yamamoto, Ngan, and

Monden 2008). In the present study, I found that genipin predominantly suppressed the levels of p-STAT3^{Tyr705} within the nucleus and survivin mRNA levels were significantly decreased in genipin-treated cells. These results suggest that reduced levels of p-STAT3^{Tyr705} within the nucleus may be responsible for the inhibition of survivin expression via transcriptional regulation.

The phosphorylation of PEST motifs in the Mcl-1 sequence renders it vulnerable to degradation by the 20S proteasome, which is mediated by multiple ubiquitin ligases, such as Mcl-1 ubiquitin ligase E3, SCF$^{\beta-TrCP}$, SCF^{FBW7}, and TRIM17. This results in phosphorylation-dependent ubiquitination and a short half-life, whereas deubiquitinases, such as USP9X, DUB3, and JOSD1, are known for mediating the restoration of Mcl-1 ubiquitination, ultimately impeding its proteasomal degradation and leading to elevated Mcl-1 stability (Senichkin et al. 2020; Senichkin et al. 2019). In the present study, the mRNA levels of Mcl-1 in HSC-4 cells were not affected by genipin treatment at 6 and 12 h, in contrast to 24 h. Therefore, I hypothesized that genipin may decrease Mcl-1 expression through a post-translational

mechanism at early time points (~12 h). To confirm this, I determined the effect of CHX or MG132 in HSC-4 cells treated with genipin. Genipin combined with CHX gradually decreased Mcl-1 expression compared with CHX treatment alone. In addition, MG132 restored the reduction of Mcl-1 induced by genipin treatment, suggesting that genipin treatment facilitates proteasomal-mediated degradation of Mcl-1 in human OSCC cells. In this regard, my results are obviously different from that of a previous report showing that genipin only affects the transcriptional activity of Mcl-1 by inhibiting the JAK2/STAT3 pathway in gastric cancer (Jo et al. 2019).

5. Conclusions

In conclusion, I discovered that genipin clearly inhibits the expression of p-STAT3^{Tyr705} and its downstream target molecules, survivin and Mcl-1, through transcriptional and/or post-translational processes, which contributes to the induction of apoptotic cell death in human OSCC cells (Fig. 11). Genipin may be effective for the treatment of human OSCC exhibiting high STAT3 kinase activity.

6. References

Aoki, Yoshiyasu, Gerald M Feldman, and Giovanna Tosato. 2003. "Inhibition of STAT3 signaling induces apoptosis and decreases survivin expression in primary effusion lymphoma." *Blood, The Journal of the American Society of Hematology* 101 (4): 1535-1542.

Baek, Seung Ho, Jeong-Hyeon Ko, Hanwool Lee, Jinhong Jung, Moonkyoo Kong, Jung-woo Lee, Junhee Lee, Arunachalam Chinnathambi, ME Zayed, and Sulaiman Ali Alharbi. 2016. "Resveratrol inhibits STAT3 signaling pathway through the induction of SOCS-1: Role in apoptosis induction and radiosensitization in head and neck tumor cells." *Phytomedicine* 23 (5): 566-577.

Boidot, R., F. Vegran, and S. Lizard-Nacol. 2014. "Transcriptional regulation of the survivin gene." *Mol Biol Rep* 41 (1): 233-40. https://doi.org/10.1007/s11033-013-2856-0.

Bowman, T., R. Garcia, J. Turkson, and R. Jove. 2000. "STATs in oncogenesis." *Oncogene* 19 (21): 2474–88. https://doi.org/10.1038/sj.onc.1203527.

Bromberg, Jacqueline F, Melissa H Wrzeszczynska, Geeta Devgan, Yanxiang Zhao, Richard G Pestell, Chris Albanese, and James E Darnell Jr. 1999. "Stat3 as an oncogene." *Cell* 98 (3): 295–303.

Carneiro, B. A., and W. S. El-Deiry. 2020. "Targeting apoptosis in cancer therapy." *Nat Rev Clin Oncol* 17 (7): 395–417. https://doi.org/10.1038/s41571-020-0341-y.

Chen, K. B., W. Yang, Y. Xuan, and A. J. Lin. 2021. "miR-526b-3p inhibits lung cancer cisplatin-resistance and metastasis by inhibiting STAT3-promoted PD-L1." *Cell Death Dis* 12 (8): 748. https://doi.org/10.1038/s41419-021-04033-8.

D'Arcy, M. S. 2019. "Cell death: a review of the major forms of apoptosis, necrosis and autophagy." *Cell Biol Int* 43 (6): 582–592. https://doi.org/10.1002/cbin.11137.

Du, G., T. Sun, Y. Zhang, H. Lin, J. Li, W. Liu, Y. Wang, B. Zhao, H. Li, and Y. Liu. 2013. "The mitochondrial dysfunction plays an

important role in urethane-induced lung carcinogenesis." *Eur J Pharmacol* 715 (1-3): 395-404. https://doi.org/10.1016/j.ejphar.2013.04.031.

Fan, Xiaofei, Lin Lin, Binxin Cui, Tianming Zhao, Lihong Mao, Yan Song, Xiaoyu Wang, Hongjuan Feng, Yu Qingxiang, and Jie Zhang. 2020. "Therapeutic potential of genipin in various acute liver injury, fulminant hepatitis, NAFLD and other non-cancer liver diseases: More friend than foe." *Pharmacological Research* 159: 104945.

Fulda, S. 2009. "Tumor resistance to apoptosis." *Int J Cancer* 124 (3): 511-5. https://doi.org/10.1002/ijc.24064.

Grandis, J. R., S. D. Drenning, Q. Zeng, S. C. Watkins, M. F. Melhem, S. Endo, D. E. Johnson, L. Huang, Y. He, and J. D. Kim. 2000. "Constitutive activation of Stat3 signaling abrogates apoptosis in squamous cell carcinogenesis in vivo." *Proc Natl Acad Sci U S A* 97 (8): 4227-32. https://doi.org/10.1073/pnas.97.8.4227.

Hanahan, D., and R. A. Weinberg. 2011. "Hallmarks of cancer: the next generation." *Cell* 144 (5): 646–74. https://doi.org/10.1016/j.cell.2011.02.013.

Horiguchi, A., T. Asano, K. Kuroda, A. Sato, J. Asakuma, K. Ito, M. Hayakawa, M. Sumitomo, and T. Asano. 2010. "STAT3 inhibitor WP1066 as a novel therapeutic agent for renal cell carcinoma." *British Journal of Cancer* 102 (11): 1592–1599. https://doi.org/10.1038/sj.bjc.6605691.

Hu, Yamei, Fangfang Liu, Xuechao Jia, Penglei Wang, Tingxuan Gu, Hui Liu, Tingting Liu, Huifang Wei, Hanyong Chen, Jiuzhou Zhao, Ran Yang, Yingying Chen, Zigang Dong, and Kangdong Liu. 2021. "Periplogenin suppresses the growth of esophageal squamous cell carcinoma in vitro and in vivo by targeting STAT3." *Oncogene* 40 (23): 3942–3958. https://doi.org/10.1038/s41388-021-01817-2.

Jo, Min Jee, Soyeon Jeong, Hye Kyeong Yun, Dae Yeong Kim, Bo Ram Kim, Jung Lim Kim, Yoo Jin Na, Seong Hye Park, Yoon A. Jeong, Bu Gyeom Kim, Hassan Ashktorab, Duane T. Smoot, Jun Young Heo, Jeongsu Han, Dae-Hee Lee, and Sang Cheul

Oh. 2019. "Genipin induces mitochondrial dysfunction and apoptosis via downregulation of Stat3/mcl-1 pathway in gastric cancer." *BMC Cancer* 19 (1): 739. https://doi.org/10.1186/s12885-019-5957-x.

Johnson, D. E., B. Burtness, C. R. Leemans, V. W. Y. Lui, J. E. Bauman, and J. R. Grandis. 2020. "Head and neck squamous cell carcinoma." *Nat Rev Dis Primers* 6 (1): 92. https://doi.org/10.1038/s41572-020-00224-3.

Johnson, Daniel E., Rachel A. O'Keefe, and Jennifer R. Grandis. 2018. "Targeting the IL-6/JAK/STAT3 signalling axis in cancer." *Nature Reviews Clinical Oncology* 15 (4): 234-248. https://doi.org/10.1038/nrclinonc.2018.8.

Jung, Y. Y., I. J. Ha, J. Y. Um, G. Sethi, and K. S. Ahn. 2022. "Fangchinoline diminishes STAT3 activation by stimulating oxidative stress and targeting SHP-1 protein in multiple myeloma model." *J Adv Res* 35: 245-257. https://doi.org/10.1016/j.jare.2021.03.008.

Kanda, Naoki, Hiroshi Seno, Yoshitaka Konda, Hiroyuki Marusawa, Masashi Kanai, Toshio Nakajima, Tomoko Kawashima,

Apichart Nanakin, Tateo Sawabu, Yoshito Uenoyama, Akira Sekikawa, Mayumi Kawada, Katsumasa Suzuki, Takahisa Kayahara, Hirokazu Fukui, Mitsutaka Sawada, and Tsutomu Chiba. 2004. "STAT3 is constitutively activated and supports cell survival in association with survivin expression in gastric cancer cells." *Oncogene* 23 (28): 4921–4929. https://doi.org/10.1038/sj.onc.1207606.

Kim, Lee-Han, Sachita Khadka, Ji-Ae Shin, Ji-Youn Jung, Mi-Heon Ryu, Hyun-Ju Yu, Hae Nim Lee, Boonsil Jang, In-Hyoung Yang, and Dong-Hoon Won. 2017. "Nitidine chloride acts as an apoptosis inducer in human oral cancer cells and a nude mouse xenograft model via inhibition of STAT3." *Oncotarget* 8 (53): 91306.

Lee, J. H., C. D. Mohan, S. Basappa, S. Rangappa, A. Chinnathambi, T. A. Alahmadi, S. A. Alharbi, A. P. Kumar, G. Sethi, K. S. Ahn, and K. S. Rangappa. 2019. "The IkappaB Kinase Inhibitor ACHP Targets the STAT3 Signaling Pathway in Human Non-Small Cell Lung Carcinoma Cells." *Biomolecules* 9 (12). https://doi.org/10.3390/biom9120875.

Li, M., F. Gao, X. Yu, Q. Zhao, L. Zhou, W. Liu, and W. Li. 2020. "Promotion of ubiquitination-dependent survivin destruction contributes to xanthohumol-mediated tumor suppression and overcomes radioresistance in human oral squamous cell carcinoma." *J Exp Clin Cancer Res* 39 (1): 88. https://doi.org/10.1186/s13046-020-01593-z.

Li, Yuan, Hong Du, Yulin Qin, Jennifer Roberts, Oscar W. Cummings, and Cong Yan. 2007. "Activation of the Signal Transducers and Activators of the Transcription 3 Pathway in Alveolar Epithelial Cells Induces Inflammation and Adenocarcinomas in Mouse Lung." *Cancer Research* 67 (18): 8494-8503. https://doi.org/10.1158/0008-5472.Can-07-0647.

Lo Muzio, L., G. Pannone, S. Staibano, M. D. Mignogna, C. Rubini, M. A. Mariggio, M. Procaccini, F. Ferrari, G. De Rosa, and D. C. Altieri. 2003. "Survivin expression in oral squamous cell carcinoma." *Br J Cancer* 89 (12): 2244-8. https://doi.org/10.1038/sj.bjc.6601402.

Macha, M. A., A. Matta, J. Kaur, S. S. Chauhan, A. Thakar, N. K. Shukla, S. D. Gupta, and R. Ralhan. 2011. "Prognostic

significance of nuclear pSTAT3 in oral cancer." *Head Neck* 33 (4): 482–9. https://doi.org/10.1002/hed.21468.

McLornan, D. P., J. E. Pope, J. Gotlib, and C. N. Harrison. 2021. "Current and future status of JAK inhibitors." *Lancet* 398 (10302): 803–816. https://doi.org/10.1016/S0140-6736(21)00438-4.

Mohammad, R. M., I. Muqbil, L. Lowe, C. Yedjou, H. Y. Hsu, L. T. Lin, M. D. Siegelin, C. Fimognari, N. B. Kumar, Q. P. Dou, H. Yang, A. K. Samadi, G. L. Russo, C. Spagnuolo, S. K. Ray, M. Chakrabarti, J. D. Morre, H. M. Coley, K. Honoki, H. Fujii, A. G. Georgakilas, A. Amedei, E. Niccolai, A. Amin, S. S. Ashraf, W. G. Helferich, X. Yang, C. S. Boosani, G. Guha, D. Bhakta, M. R. Ciriolo, K. Aquilano, S. Chen, S. I. Mohammed, W. N. Keith, A. Bilsland, D. Halicka, S. Nowsheen, and A. S. Azmi. 2015. "Broad targeting of resistance to apoptosis in cancer." *Semin Cancer Biol* 35 Suppl: S78–S103. https://doi.org/10.1016/j.semcancer.2015.03.001.

Mohan, C. D., S. Rangappa, H. D. Preetham, S. Chandra Nayaka, V. K. Gupta, S. Basappa, G. Sethi, and K. S. Rangappa. 2022.

"Targeting STAT3 signaling pathway in cancer by agents derived from Mother Nature." *Semin Cancer Biol* 80: 157–182. https://doi.org/10.1016/j.semcancer.2020.03.016.

Senichkin, V. V., A. Y. Streletskaia, A. S. Gorbunova, B. Zhivotovsky, and G. S. Kopeina. 2020. "Saga of Mcl-1: regulation from transcription to degradation." *Cell Death Differ* 27 (2): 405–419. https://doi.org/10.1038/s41418-019-0486-3.

Senichkin, V. V., A. Y. Streletskaia, B. Zhivotovsky, and G. S. Kopeina. 2019. "Molecular Comprehension of Mcl-1: From Gene Structure to Cancer Therapy." *Trends Cell Biol* 29 (7): 549–562. https://doi.org/10.1016/j.tcb.2019.03.004.

Shanmugam, M. K., H. Shen, F. R. Tang, F. Arfuso, M. Rajesh, L. Wang, A. P. Kumar, J. Bian, B. C. Goh, A. Bishayee, and G. Sethi. 2018. "Potential role of genipin in cancer therapy." *Pharmacol Res* 133: 195–200. https://doi.org/10.1016/j.phrs.2018.05.007.

Siveen, K. S., S. Sikka, R. Surana, X. Dai, J. Zhang, A. P. Kumar, B. K. Tan, G. Sethi, and A. Bishayee. 2014. "Targeting the STAT3 signaling pathway in cancer: role of synthetic and

natural inhibitors." *Biochim Biophys Acta* 1845 (2): 136–54. https://doi.org/10.1016/j.bbcan.2013.12.005.

Sun, L., Y. Yan, H. Lv, J. Li, Z. Wang, K. Wang, L. Wang, Y. Li, H. Jiang, and Y. Zhang. 2022. "Rapamycin targets STAT3 and impacts c–Myc to suppress tumor growth." *Cell Chem Biol* 29 (3): 373–385 e6. https://doi.org/10.1016/j.chembiol.2021.10.006.

Sun, S., Y. Wu, W. Guo, F. Yu, L. Kong, Y. Ren, Y. Wang, X. Yao, C. Jing, C. Zhang, M. Liu, Y. Zhang, M. Zhao, Z. Li, C. Wu, Y. Qiao, J. Yang, X. Wang, L. Zhang, M. Li, and X. Zhou. 2018. "STAT3/HOTAIR Signaling Axis Regulates HNSCC Growth in an EZH2–dependent Manner." *Clin Cancer Res* 24 (11): 2665–2677. https://doi.org/10.1158/1078–0432.CCR–16–2248.

Tang, Daolin, Rui Kang, Tom Vanden Berghe, Peter Vandenabeele, and Guido Kroemer. 2019. "The molecular machinery of regulated cell death." *Cell Research* 29 (5): 347–364. https://doi.org/10.1038/s41422–019–0164–5.

Tower, John. 2015. "Programmed cell death in aging." *Ageing research reviews* 23: 90–100.

Tu, Y., Y. Zhong, J. Fu, Y. Cao, G. Fu, X. Tian, and B. Wang. 2011. "Activation of JAK/STAT signal pathway predicts poor prognosis of patients with gliomas." *Med Oncol* 28 (1): 15–23. https://doi.org/10.1007/s12032-010-9435-1.

Wei, M., Y. Wu, H. Liu, and C. Xie. 2020. "Genipin Induces Autophagy and Suppresses Cell Growth of Oral Squamous Cell Carcinoma via PI3K/AKT/MTOR Pathway." *Drug Des Devel Ther* 14: 395–405. https://doi.org/10.2147/DDDT.S222694.

Wheatley, Sally P, and Dario C Altieri. 2019. "Survivin at a glance." *Journal of Cell Science* 132 (7): jcs223826.

Yamamoto, H., C. Y. Ngan, and M. Monden. 2008. "Cancer cells survive with survivin." *Cancer Sci* 99 (9): 1709–14. https://doi.org/10.1111/j.1349-7006.2008.00870.x.

Yang, P. L., L. X. Liu, E. M. Li, and L. Y. Xu. 2020. "STAT3, the Challenge for Chemotherapeutic and Radiotherapeutic

Efficacy." *Cancers (Basel)* 12 (9). https://doi.org/10.3390/cancers12092459.

Yao, M. L., J. Gu, Y. C. Zhang, N. Wang, Z. H. Zhu, Q. T. Yang, M. Liu, and J. F. Xia. 2015. "[Inhibitory effect of Genipin on uncoupling protein-2 and energy metabolism of androgen-independent prostate cancer cells]." *Zhonghua Nan Ke Xue* 21 (11): 973-6.

You, Z., D. Xu, J. Ji, W. Guo, W. Zhu, and J. He. 2012. "JAK/STAT signal pathway activation promotes progression and survival of human oesophageal squamous cell carcinoma." *Clin Transl Oncol* 14 (2): 143-9. https://doi.org/10.1007/s12094-012-0774-6.

Zheng, Q., H. Dong, J. Mo, Y. Zhang, J. Huang, S. Ouyang, S. Shi, K. Zhu, X. Qu, W. Hu, P. Liu, Y. Wang, and X. Zhang. 2021. "A novel STAT3 inhibitor W2014-S regresses human non-small cell lung cancer xenografts and sensitizes EGFR-TKI acquired resistance." *Theranostics* 11 (2): 824-840. https://doi.org/10.7150/thno.49600.

국 문 초 록

구강 편평상피세포암종에서 STAT3 신호전달을 억제하는 genipin의 항암 효능에 관한 연구

박 동 국

서울대학교 대학원

치의과학과 구강병리학 전공

지도 교수: 조 성 대

1. 목 적: 이전 연구에 따르면 제니핀 (genipin)은 구강 편평상피세포암종 (OSCC)을 포함하는 여러 유형의 암에 대해 세포 독성이 있는 것으로 알려져 있다. 하지만, 구강 편평상피세포암종 세포주에서 제니핀의 항암 효능을 설명하는 메커니즘은 현재까지 미미한 실정이다. 본 연구는 구강 편평상피세포암종 세포주에서 제니핀이 유도하는 항암 효능의 근본적인 메커니즘을 규명하는 것을 목표로 한다.

2. 재료 및 방 법: 구강 편평상피세포암종에서 제니핀의 세포증식 억제 효과는 Cell Counting Kit-8, soft agar 및 세포주 유래 이종 이식 동물모델을 통해 평가되었다. 또한, 세포사멸 (apoptotic cell death)을 유도하는 제니핀의 효능은 DAPI staining을 통한 핵의 형태학적 변화, sub-G1 분석, Annexin V/PI double staining 과 cleaved PARP 및 cleaved caspase 3 단백질의 검출을 통해 평가되었다. 제니핀에 의해 매개되는 signal transduction and activator of transcription 3 (STAT3)의 활성억제 메커니즘은 western blotting, subcellular fractionation of the nucleus and cytoplasm, immunocytochemistry 와 quantitative real-time PCR을 통해 STAT3의 타겟 유전자들의 발현을 확인하였다.

3. 결 과 및 고찰: 제니핀은 in virto 및 in vivo에서 구강 편평상피세포암종에서 세포증식 억제했다. 또한 제니핀은 cleaved PARP 과 cleaved caspase 3단백질 발현을 농도의존적으로 증가시켰으며, pan-caspase 억제제인 Z-VAD-FMK를 처리함으로써, 제니핀에 의한 세포 사멸이 caspase 3에 의존적인 경로를 통하여 유도되는 것을 확인하였다. Subcellular fractionation 과 immunocytochemistry를 통해 제니핀이 핵에 존재하는 p-

STAT3(Y705)의 발현을 농도의존적으로 감소시키는 것을 확인하였다. 또한, 제니핀에 의한 p-STAT3(Y705) 발현의 억제는 세포 사멸에 연관된 단백질인 survivin 과 myeloid cell leukemia-1 (Mcl-1) 발현의 감소를 초래했다. 제니핀에 의해 매개되는 survivin 및 Mcl-1 발현의 감소는 전사 및/또는 번역 후 조절 메커니즘에 의해 발생했으며, 이는 세포 맥락에 의존적인 방식으로 발생했다. 이 연구로, 제니핀이 구강 편평상피세포암종에서 STAT3의 활성을 억제하고 타겟 유전자들의 발현을 감소시킴으로써 세포사멸을 유도할 수 있는 항암 효능을 제시하였다.

주요어: 제니핀; Signal transduction and activator of transcription 3; 구강 편평상피세포암종; 세포사멸; Myeloid cell leukemia-1; Survivin

학 번: 2021-25862